VIA MEDICA

Original article

NOWOTWORY Journal of Oncology
2022, volume 72, number 2, 67–73
DOI: 10.5603/NJO.a2022.0013

ISSN 0029–540X, e-ISSN: 2300-2115
www.nowotwory.edu.pl

Dose estimation in patients treated with radiotherapy for SARS-COVID disease based on EPID measurement

Krzysztof Ślosarek[1, 2], Tomasz Rutkowski[1], Adam Gądek[1], Łukasz Sroka[1], Łukasz Dolla[1], Roman Rutkowski[1, 2], Jerzy Jaroszewicz[3]

[1]*National Research Institute of Oncology, Gliwice Branch, Gliwice, Poland*
[2]*Varian Medical Systems, Warsaw, Poland*
[3]*Department of Infectious Diseases and Hepatology, Medical University of Silesia, Katowice, Poland*

Introduction. COVID radiotherapy requires performance of all radiotherapy (RT) procedures during one site visit due to the infectious nature of the disease. The aim of the study was to develop methods of estimating the delivered dose based on electronic portal image device (EPID) signal during treatment.

Material and methods. Electronic portal image device signal was measured as a function of the phantom dose. The dose in 14 COVID patients was estimated for two X6MV beams.

Results. The method allows to estimate dose in phantom with uncertainty of 12%. In this case, a systematic error was reported. Therefore, coefficients for clinical data were calculated and used to determine the dose in patients. The mean difference between the dose calculated and the dose measured for the 14 patients was 1%, but the uncertainty of this method was estimated as ±6%

Conclusions. The proposed method may be useful in clinical practice as *in vivo* method. However, due to high uncertainty, it should be dedicated to the detection of "big" errors.

Key words: SARS-COVID, EPID, fluence map, QA, *in vivo* dosimetry

Introduction

In December 2020, the National Research Institute of Oncology in Poland, Gliwice Branch, began the irradiation of SARS-COVID patients [1, 2]. A dose of 1 Gy was scheduled to the lung volume. This was part of a II phase study performed on 14 patients hospitalized between December 2020 and April 2021 due to severe viral pneumonia over the course of COVID-19 in the Department of Infectious Diseases and Hepatology, Medical University of Silesia, Bytom, Poland. There were 5 females and 9 men with a median age of 66 years (range 49–78). All of them required continuous oxygen supplementation. Inclusion criteria consisted of COVID-19 infection confirmed by polymerase chain reaction (PCR), age ≥18 years, Zubrod score ≤3 points, clinical and radiological (radiography [RTG] or high resolution computed tomography [HRCT]) signs of viral pneumonia, severe COVID-19 – stage 3 according to national guidelines with SpO_2 < 90% and the need for oxygen supplementation the ability for providing of concise consent. Among the exclusion criteria were acute respiratory distress syndrome (ARDS), the need for invasive or mechanical ventilation, pregnancy,

How to cite:

Ślosarek K, Rutkowski T, Gądek A, Sroka Ł, Dolla Ł, Rutkowski R., Jaroszewicz J. ***Dose estimation in patients treated with radiotherapy for SARS-COVID disease based on EPID measurement.*** *NOWOTWORY J Oncol* 2022; 72: 67–73.

any thorax malignancy in the last 5 years, contraindication for medical transport for low dose radiotherapy (LDRT) procedure, cognitive impairment and therapy with another experimental therapies. The study was conducted according to the guidelines of the Declaration of Helsinki, and approved by the Ethics Committee of the Maria Sklodowska-Curie National Research Institute of Oncology, Gliwice Branch, Poland; all participants gave written informed consent. RT administered at LDRT modulates the inflammatory response. This anti-inflammatory action of LDRT includes various mechanisms including the induction of apoptosis in immune cells, decreasing levels of some proinflammatory cytokines, inhibiting leukocyte recruitment and the reducing function of macrophages (Arenas). This feature of LDRT was discovered and clinically utilized in the first half of the 20th century prior to the era of antibiotics in the treatment of a wide range of inflammatory and infectious diseases such as sinusitis, arthritis, gas gangrene, carbuncles, inner ear infections, including pneumonia (Calabrese) [22, 23]. Due to the above facts, the concept of utilizing LDRT as a suppressor of COVID-19 related pneumonia was raised.

The radiotherapy linear accelerator TrueBeam manufactured by Varian equipped with as1200 EPID was used. As the TPS treatment planning system ECLIPSE (Varian), version 16.1, was used. During the irradiation/tratment of SARS-COVID patients, it was presumed that the following assumptions should be followed:

- the duration of the procedure should be minimized,
- the number of persons in direct contact with the patient should be minimal,
- all Radiotherapy Trials Quality Assurance (RT QA) requirements must be met.

This must be done during a one-off radiotherapy session. An important part of the RT QA procedures is the full control of the delivered dose. This task is difficult to accomplish because the standard treatment "planning path" does not exist here. The patient has no stabilization and no 3DCT imaging. All procedures of "treatment planning" and QA are carried out in a treatment room. An irradiation technique should be simple. Two opposite fields with multi-leaf collimators (MLC) were selected. The irradiation time of the 1 Gy dose was calculated for a depth of half of the AP dimension. For a beam angle 0° and 180°, a dose of 0.5 Gy was planned. This procedure is also used for palliative cases. The main question of this study was: Is it possible to verify the delivered dose during a single session?

The fluence map obtained with EPID was tested to measure the dose in real time [3–5], repeated treatment [6–9], point dose measurement [10] and dose distribution [11–14]. Fluence maps were also used to verify the correct operation of the MLC [15–18] or compatibility with the planned dose distribution [19]. EPID can be used as a dose meter in *in vivo* dosimetry [20, 21]. For this purpose, cone-beam computed tomography (CBCT) and EPIDs are excellent tools. A 3D image is obtained with CBCT and an EPID is used to acquire a fluence map during a therapeutic session to estimate a dose. The aim of the study was to develop a method of measuring the dose during a therapeutic session using the EPID.

Material and methods

Irradiation is carried out by two opposite X-6MV fields. A 1 Gy dose is defined at a point at a depth of ½ of the AP dimension in the geometric center of the right field beam (right lung). The irradiation time was calculated for this depth using the Eclipse Irreg module [1, 2]. These calculations do not take into account tissue density and are based only on dose depth, beam specification and source to surface distance (SSD) dimensions. In the case, the calculated dose may be overstated as the density of the lung tissue is less than the density of water. After a therapeutic session a CBCT is acquired. It is used

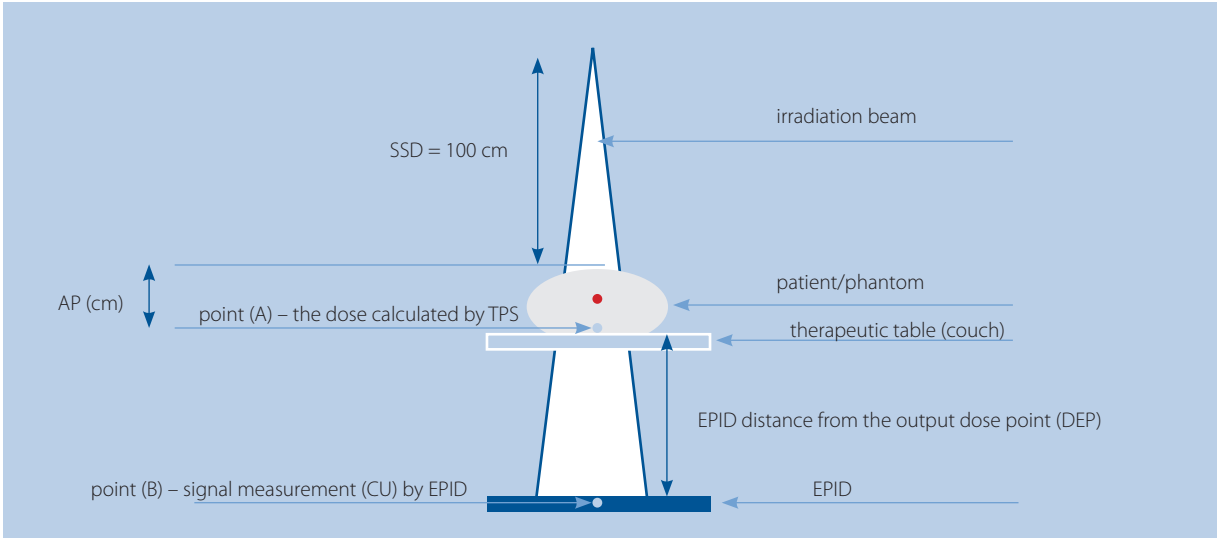

Figure 1. Patient dose estimation diagram based on EPID signal measurement. Knowing the patient's AP dimension, the distance of the output dose point from the EPID can be calculated

to calculate the 3D distribution of the dose for the previously calculated irradiation time. During irradiation a fluence map is measured by an EPID. This signal can be correlated with the dose (fig. 1).

If "A" is selected close to the exit of the beam, then the output dose takes into account the absorption of radiation. The radiation absorption through the couch can be omitted and the output dose can be correlated at "A" with the EPID signal "B". The higher the dose at "A", the greater measured signal. EPID calibration should be carried out to correlate signal (CU) and radiation dose (Gy) dependency.

The next step is to determine the dependence of the signal of dose on the distance between "A" and "B". It is assumed that the greater this distance, the smaller the measured signal if the dose at "A" is constant. Measurements were made for SSD = 90, 100 and 110 cm. The position of the EPID was set at 160 cm. The phantom is 20 cm thick, changing the SSD changes the distance between "A" and "B"; DEP – distance EPID point "A". These distances are: 50, 40 and 30 cm for SSD: 90, 100 and 110 cm. At a depth of ½ AP of the phantom, the following doses were defined: 0.5, 1.0 and 1.5 Gy, for a 10 x 10 cm beam. The dose at "A", "A1" and "A2" are due to different effective depths because the CIRS (Computerized Imaging Reference Systems, Inc., IMRT Thorax Phantom Model 002LFC) measurement phantom has a heterogeneous density (fig. 2).

The calculated doses at "A", "A1" and "A2" will take dependencies into account. In order to confirm the dose calculation model based on the EPID, a "blank test" was performed.

This method was used for 14 patients with SARS-COVID. Images (MV, kV) were taken to determine the AP dimension and define the irradiated volume by determining the MLC shape. Based on the AP dimension and the shape of fields, the irradiation time was calculated for 1 Gy using the Irreg module. The middle of the AP dimension was situated in the middle of the left lung beam. The Irreg module calculates irradiation time based on the depth for 1 g/cm^3 density for the defined dimension of the field. After irradiation, a CBCT imaging was performed to determine the density and to define treated volumes and critical organs. The shape of the irradiation fields was copied onto the acquired 3DCBCT. 3D radiation dose distribution calculations were performed using the ECLIPSE Acuros algorithm v 16.1 [1, 2]. Dose output points were selected for field 0° and 180°. Four points were obtained to compare the

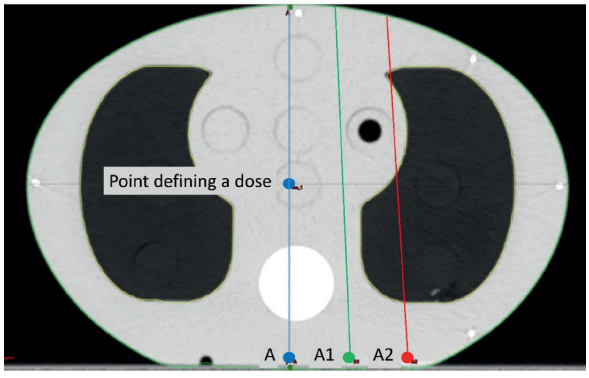

Figure 2. Phantom and points "A", "A1" and "A2" location for which the doses used for EPID calibration as a function of distance were calculated. Equivalent depths should be 21.5 cm, 19.3 cm and 12.1 cm respectively for points "A", "A1" and "A2". The difference in these depths is related to the densities through which the beam's "radius" passes

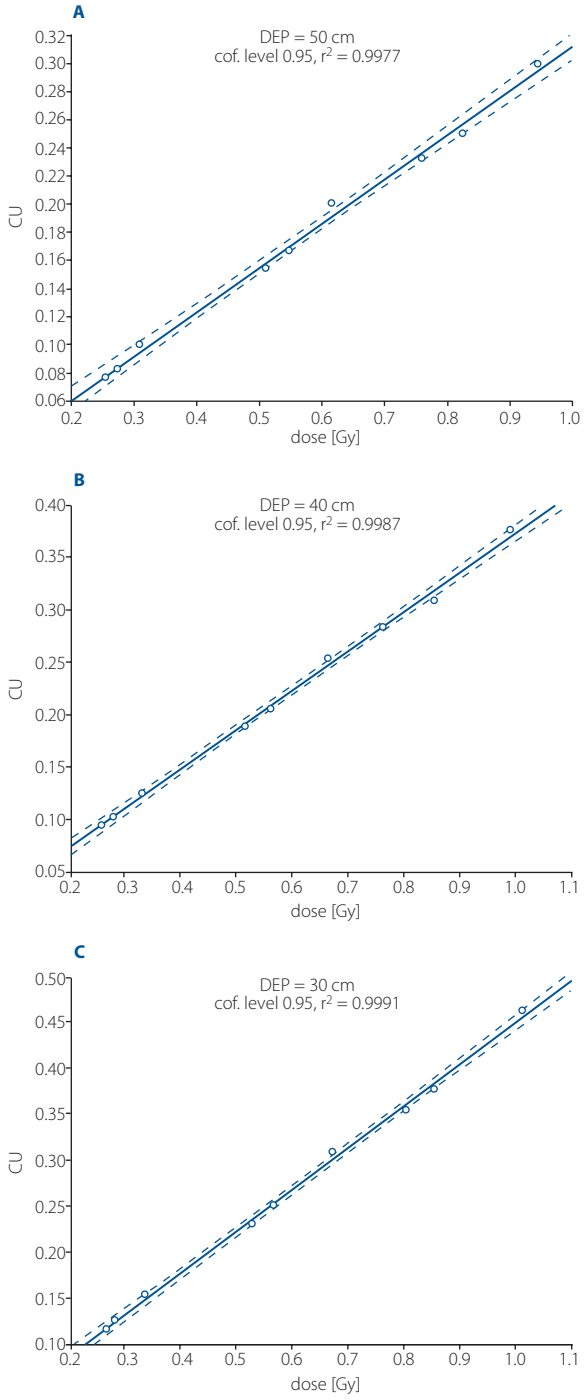

Figure 3. Relationship between the EPID signal (CU) and the output dose for different therapeutic table distances from the EPID: A 50 cm, B 40 cm and C 30 cm. The straight directional coefficient depends on the DEP, and the correlation coefficients for all DEP are above 0.99

measured and calculated doses. These points were selected in the homogeneous dose volume. These single measurement points can be subject to great uncertainty, therefore average values, from four points, were analyzed.

To assess the conformity of the calculated and measured values, non-parametric tests such as the Wilcoxon signed-rank test were used, taking a p value less than 0.05 as the level of statistical significance.

Results

The dependence of the EPID value on the value of the output dose was measured. In the dose range from 0.15 Gy to 0.9 Gy, a linear relationship ($r^2 = 0.99$) was found between the output dose (phantom) and the signal value (EPID–CU). The next stage involved measuring the EPID signal at a distance from the position of the therapeutic table for different output dose values. Figure 3 shows the results of the EPID signal dependency on different distances from the therapeutic table and different output doses.

The measurements showed a linear relationship of 0.95 confidence for a correlation coefficient above 0.99. On this basis, a directional factor "K" could be determined for the DEP dependency (EPID distance from the output dose):

$$\text{Dose [Gy]} = \text{CU} \times K(\text{DEP}) \quad [1]$$

The calculations showed the following values of the coefficient "K": 3.2106 for DEP = 50 cm, 2.6871 for DEP = 40 cm, 2.2304 for DEP = 30 cm. These dependencies describe an exponential function:

$$K(\text{DEP}) = a \times \exp(b \times \text{DEP}) \quad [2]$$

The least squared method was used to calculate coefficients "a" and "b", which were equal to: 1.2932 and 0.0182. The correlation coefficient of the match was above 0.99.

The sets of "K" coefficients obtained from the measurements were then compared:

$$K(\text{DEP}) = \text{dose [Gy] outlet} / \text{CU (measured)} \quad [3]$$

and contrasted with the "K" factor calculated from formula [2], for the calculated coefficients "a" and "b". The Wilcoxon test was used to compare the results, which did not show statistically significant differences between them ($p > 0.05$).

A blank evaluation of the output dose was performed, based on the CU measurement, to validate the developed model. The dose should have been estimated at the defined point (fig. 2). The EPID signal was read as described before. Since the dose was defined in the middle of the AP dimension of the phantom, it was necessary to introduce a relationship between the point of its definition and the point of the output dose. The % depth dose (%DD) value was used for the equivalent depth and read from the dose distribution. This approach is consistent with the actual dose estimation conditions for treated patients. The results of the comparison are presented in table I.

The mean dose differences – measured and calculated for "A", "A1" and "A2" were: 0.75% for SSD = 100 cm, 1.97% for SSD = 110 cm, and 1.22% for SSD = 90 cm. Doses were compared using the Wilcoxon test. No differences were reported between them, which would have been statistically significant ($p = 0.5165$). It can be assumed that it is possible to estimate the dose (in a phantom) based on EPID signal measurements. Table I shows that the maximum difference between the calculated and measured doses was 5.56%, and it was found that the method of estimating the dose based on EPID was subject to uncertainty of 12% (±5.56%).

The developed method was used to estimate the dose received by irradiated SARS-COVID patients. Figure 4 shows the points that were selected to estimate the dose and the geometry of the measurement.

Table I. Doses calculated by the treatment planning system and estimated based on the EPID signal measurement. Model validation conditions on the measurement phantom for geometry is similar to the patient's irradiation conditions

SSD [cm]	Measurement point	CU read from EPID	DEP [cm]	Measured output dose [Gy]	% of output dose	Measured dose [Gy]	Dose [Gy] calculated by TPS	% Diff.
100	A	0.1446	40	0.3887	53.6	0.73	0.75	–3.30%
100	A1	0.1539	40	0.4137	56.3	0.73	0.75	–2.02%
100	A2	0.1876	40	0.5043	63.7	0.79	0.75	5.56%
110	A	0.4713	30	1.0562	54.9	1.92	2	–3.76%
110	A1	0.5046	30	1.1308	58.5	1.93	2	–3.34%
110	A2	0.6136	30	1.3750	67.4	2.04	2	2.06%
90	A	0.1945	50	0.6272	52.0	1.21	1.25	–3.50%
90	A1	0.2093	50	0.6750	55.3	1.22	1.25	–2.29%
90	A2	0.2449	50	0.7898	63.8	1.24	1.25	–0.96%

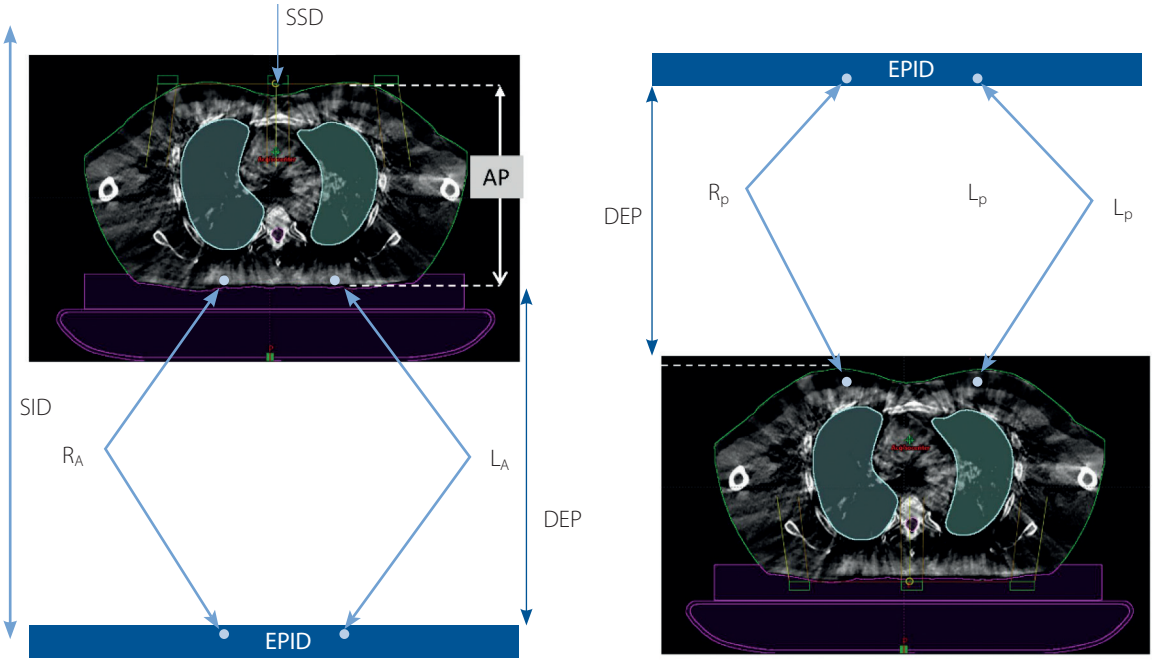

Figure 4. Geometry for measuring the CU value on the basis of which the dose is calculated. SSD = 100 cm, for each irradiation field, and SID (EPID setting) = 160 cm (or 150 cm). DEP depends on the AP dimension of the patient

Table II. The comparison of measured (EPID) and calculated (TPS) doses. %Δ is the mean difference for the four measuring points: R_A, L_A, R_P, and L_P, calculated as: 100% x ($EPID_{dose}$ –TPS_{dose})/TPS_{dose}.

Beam angle [deg]	Measurement point	Fluence [CU]	Dose measured by EPID [Gy]	Dose [Gy] calculated by TPS	Mean %Δ	AP [cm] Patient's dimension	DEP [cm]	EPID Vertical position – SID [cm]
0	R_A	0.1774	0.332193	0.3423	7.14%	29.66	20.34	150
	L_A	0.1573	0.294554	0.3376			20.34	
180	R_P	0.1623	0.303917	0.337			20.34	
	L_P	0.1544	0.289124	0.298246			20.34	

Table II shows the results of the measured EPID dose for one of the patients. The results, for all patients, indicate that all measured doses were lower than the calculated average of 12%. Only 4 out of 14 measurements were within the uncertainty level (<12%). The Wilcoxon test showed statistically significant differences ($p < 0.05$) between the set of calculated and measured doses. Shifting the result of this measurement in one direction indicates a systematic error.

The measured dose was lower than planned for all studied patients. The geometry of the dose measurement using a phantom is different than in the case of patient irradiation e.g., patient dimensions vs phantom dimension. The EPID calibration was performed for a 10 x 10 cm beam, the actual dimension of the irradiation beam was 22 x 25 cm.

The dose output was correlated with the EPID signal for the relationship received from the clinical data using the same method as the phantom. The coefficients "a" and "b" from formula 2 were recalculated and values were obtained: a = 1.4405 and b = 0.0191. Based on these coefficient values, differences between the measured and calculated dose were found to be below 6% (except for one patient). This value falls within the uncertainty of the method estimated at ±6%. The mean difference for all patients between the calculated and measured doses was less than 1% (tab. III).

The Wilcoxon's statistical tests did not show statistically significant differences between the sets of calculated and measured doses ($p = 0.8937$).

Discussion

With regard to clinical dosimetry, in order to calculate the right dose for patients a method needs to be developed. This path determines all necessary factors that are used in clinical practice. It is necessary to explain why the described method allowed for dose estimation in the phantom model based on the EPID signal and showed a systematic error in the calculated dose when used in the patient model.

Figure 5 shows the relationship between the calculated dose and the EPID signal measured under phantom and pa-

Table III. Mean values (points R_A, L_A, R_P, L_P) of the calculated and measured doses. The differences between them are much smaller than in the case of calculations based on the coefficients obtained from phantom measurements

Patient	Mean measured dose [Gy] by EPID	Mean calculated dose [Gy] by TPS	Mean %Δ
1	0.3542	0.3475	2.36%
2	0.3875	0.3700	–4.50%
3	0.3100	0.2913	–5.92%
4	0.2695	0.2560	–4.18%
5	0.2325	0.2407	4.25%
6	0.3825	0.3912	2.44%
7	0.3115	0.3082	0.13%
8	0.3288	0.3463	5.43%
9	0.3775	0.3780	0.27%
10	0.3528	0.3306	–6.00%
11	0.2032	0.2296	13.25%
12	0.3014	0.2946	–2.22%
13	0.2709	0.2825	5.15%
14	0.3514	0.3551	1.34%

tient. It can be seen that the r^2 factor has different values, which indicates a greater dispersion of measuring points in clinical conditions. This shows that in clinical practice the uncertainty of the described method is greater. Not all phenomena associated with patient irradiation were included in the phantom model.

The selection of the CU point from the fluence map is highly uncertain and coordinates do not fully match the position of the output dose. Beam divergence is not taken into account. Phantom measurements are made for a 10 x 10 cm beam field. By correcting the field size – the output factor from TPS, the difference between the 10 x 10 cm and 25 x 25 cm field amounting to 6% – the consistency between the doses would improve, reducing the mean difference from 12% to 9%. There is also a diffused radiation issue. The performed phantom measurements allow for the determination of coefficients that can be used to calculate the dose in a patient. It needs to be remembered that there is more than 12% uncertainty, and the result is only for evaluating whether a big mistake was made. Despite the differences in the measurement geometry, the developed method of correlating the CU signal with the dose for clinical data was applied. When deciding to use an EPID in estimating the dose, the described procedure seems justified. Measurements need to be done on a phantom to prepare a method. For the "first" patients, the values calculated for a phantom should be used, taking into account the uncertainty of 12%. It is an estimate of the dose the patient receives rather than its accurate measurement. As the number of patients increases, the factors used in this method can be derived from

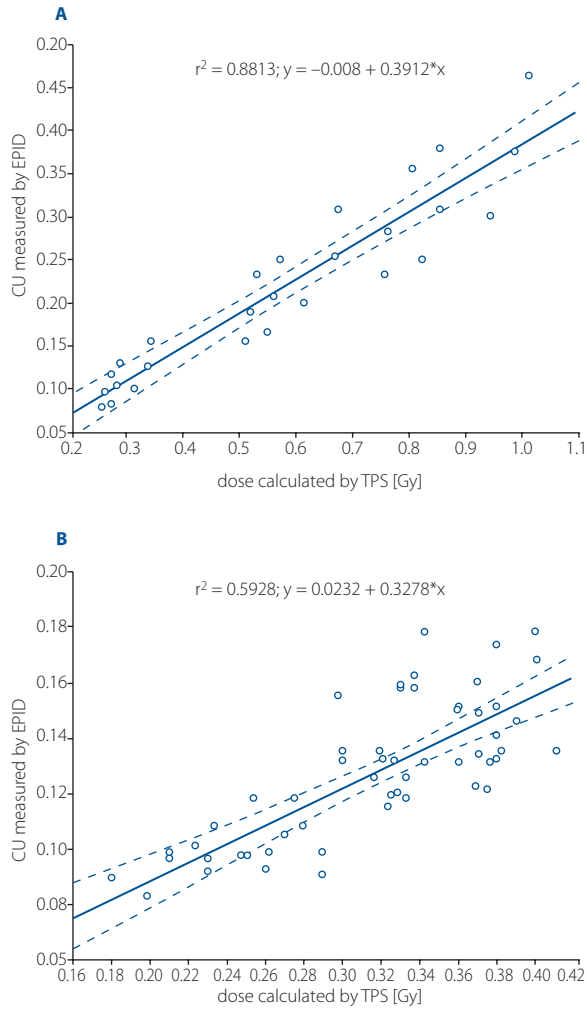

Figure 5. Relationship between the outlet dose calculated by TPS and the signal measured by the EPID for a phantom (A) and treated patients (B). It can be seen that there are differences between the directional coefficients of the two straight lines and a greater dispersion of the measurement points in clinical conditions

clinical data. This method makes it possible to estimate the dose with a measurement uncertainty of 6%.

When IMRT, VMAT were not used in RT, *in vivo* dosimetry was widely utilized [21]. The question arises: should we use the presented method? Direct contact with the patient during an irradiation session is minimized, the presence of physicists measurements does not seem to be justified. The instruments and meters used for these measurements would require sterilization due to special COVID treatment conditions. The delivery of a dose of 1 Gy should not induce negative radiation effects. The dose verification is an additional procedure. The proposed method of using an EPID does not compromise the irradiation process. This is the only method that can be used without extending the irradiation session time.

Electronic portal image device as a dose measurement system was studied [3, 10, 12]. Publications show the possibilities of EPID in dose estimation [3, 21]. Based on dynamic techniques [4, 7, 8], the comparison of fluence maps is an optimal way

of assessing the calculated dose and its real distribution. This comparison is not about one point, but the matrix of points. Measuring a matrix (a fluence map) reduces measurement uncertainty. There is no commercial solution that would estimate patient's volume dose based on a fluence map. The proposed method is burdened with uncertainty of 12%, but it is possible to use it in clinical conditions for estimating "big errors". For SARS-COVID patients, information about the received dose of radiation is useful. Further work will be carried out in the direction of using a larger number of points for reading the signal.

Conclusions

The method of dose estimation based on EPID signal measurement allows for its application in clinical practice only under certain conditions. It must be prepared in advance using phantom measurements and validated by the measurement data of real patients. Its uncertainty is within 12% and it should be treated as a method of detecting a "gross" dosimetry error.

Conflict of interest: none declared

Roman Rutkowski
National Research Institute of Oncology
Gliwice Branch
Wybrzeże Armii Krajowej 14
44-101 Gliwice, Poland
e-mail: roman.rutkowski@io.gliwice.pl

Received: 26 Aug 2021
Accepted: 20 Jan 2022

References

1. Sroka Ł, Gądek A, Dolla Ł, et al. Przeciwzapalne napromienianie płuc chorych na COVID-19. Inżynier i Fizyk Medyczny. 2021; 10(2).
2. Ślosarek K, Gądek A, Sroka Ł, et al. Lung volume irradiation procedures in patients with pneumonia during COVID-19 infection – physical aspects of treatment planning and dosimetry. Nowotwory. Journal of Oncology. 2021; 71(4): 238–242, doi: 10.5603/njo.2021.0042.
3. van Elmpt W, McDermott L, Nijsten S, et al. A literature review of electronic portal imaging for radiotherapy dosimetry. Radiother Oncol. 2008; 88(3): 289–309, doi: 10.1016/j.radonc.2008.07.008, indexed in Pubmed: 18706727.
4. Celi S, Costa E, Wessels C, et al. EPID based in vivo dosimetry system: clinical experience and results. J Appl Clin Med Phys. 2016; 17(3): 262–276, doi: 10.1120/jacmp.v17i3.6070, indexed in Pubmed: 27167283.
5. van Elmpt W, Nijsten S, Mijnheer B, et al. The next step in patient-specific QA: 3D dose verification of conformal and intensity-modulated RT based on EPID dosimetry and Monte Carlo dose calculations. Radiother Oncol. 2008; 86(1): 86–92, doi: 10.1016/j.radonc.2007.11.007, indexed in Pubmed: 18054102.
6. Klimas A, Grządziel A, Plaza D, et al. EPID – a useful interfraction QC tool. Polish Journal of Medical Physics and Engineering. 2019; 25(4): 221–228, doi: 10.2478/pjmpe-2019-0029.
7. Kruszyna-Mochalska M. EPID-based daily verification of reproducibility of patients' irradiation with IMRT plans. Rep Pract Oncol Radiother. 2018; 23(5): 309–314, doi: 10.1016/j.rpor.2018.05.003, indexed in Pubmed: 30108458.
8. Ślosarek K, Plaza D, Nas A, et al. Portal dosimetry in radiotherapy repeatability evaluation. J Appl Clin Med Phys. 2021; 22(1): 156–164, doi: 10.1002/acm2.13123, indexed in Pubmed: 33314643.
9. van Elmpt W, Petit S, De Ruysscher D, et al. 3D dose delivery verification using repeated cone-beam imaging and EPID dosimetry for stereotactic body radiotherapy of non-small cell lung cancer. Radiother Oncol. 2010; 94(2): 188–194, doi: 10.1016/j.radonc.2009.12.024, indexed in Pubmed: 20083317.
10. Slosarek K, Szlag M, Bekman B, et al. EPID in vivo dosimetry in RapidArc technique. Rep Pract Oncol Radiother. 2010; 15(1): 8–14, doi: 10.1016/j.rpor.2010.01.003, indexed in Pubmed: 24376916.
11. McDermott LN, Wendling M, Nijkamp J, et al. 3D in vivo dose verification of entire hypo-fractionated IMRT treatments using an EPID and cone-beam CT. Radiother Oncol. 2008; 86(1): 35–42, doi: 10.1016/j.radonc.2007.11.010, indexed in Pubmed: 18061692.
12. Miri N, Keller P, Zwan BJ, et al. EPID-based dosimetry to verify IMRT planar dose distribution for the aS1200 EPID and FFF beams. J Appl Clin Med Phys. 2016; 17(6): 292–304, doi: 10.1120/jacmp.v17i6.6336, indexed in Pubmed: 27929502.
13. Wendling M, Louwe RJW, McDermott LN, et al. Accurate two-dimensional IMRT verification using a back-projection EPID dosimetry method. Med Phys. 2006; 33(2): 259–273, doi: 10.1118/1.2147744, indexed in Pubmed: 16532930.
14. van Zijtveld M, Dirkx MLP, de Boer HCJ, et al. 3D dose reconstruction for clinical evaluation of IMRT pretreatment verification with an EPID. Radiother Oncol. 2007; 82(2): 201–207, doi: 10.1016/j.radonc.2006.12.010, indexed in Pubmed: 17287039.
15. Lim SB, Zwan BJ, Lee D, et al. A novel quality assurance procedure for trajectory log validation using phantom-less real-time latency corrected EPID images. J Appl Clin Med Phys. 2021; 22(3): 176–185, doi: 10.1002/acm2.13202, indexed in Pubmed: 33634952.
16. Alves VG, Ahmed M, Aliotta E, et al. An error detection method for real-time EPID-based treatment delivery quality assurance. Med Phys. 2021; 48(2): 569–578, doi: 10.1002/mp.14633, indexed in Pubmed: 33314247.
17. McCowan PM, Rickey DW, Rowshanfarzad P, et al. An investigation of gantry angle data accuracy for cine-mode EPID images acquired during arc IMRT. J Appl Clin Med Phys. 2014; 15(1): 4507, doi: 10.1120/jacmp.v15i1.4507, indexed in Pubmed: 24423849.
18. Defoor DL, Vazquez-Quino LA, Mavroidis P, et al. Anatomy-based, patient-specific VMAT QA using EPID or MLC log files. J Appl Clin Med Phys. 2015; 16(3): 5283, doi: 10.1120/jacmp.v16i3.5283, indexed in Pubmed: 26103490.
19. van Zijtveld M, Dirkx MLP, de Boer HCJ, et al. Dosimetric pre-treatment verification of IMRT using an EPID; clinical experience. Radiother Oncol. 2006; 81(2): 168–175, doi: 10.1016/j.radonc.2006.09.008, indexed in Pubmed: 17055604.
20. Grządziel A, Smolińska B, Rutkowski R, et al. EPID dosimetry – configuration and pre-treatment IMRT verification. Reports of Practical Oncology & Radiotherapy. 2007; 12(6): 307–312, doi: 10.1016/s1507-1367(10)60069-7.
21. Essers M, Mijnheer B. In vivo dosimetry during external photon beam radiotherapy. Int J Radiat Biol. 1999; 43(2): 245–259, doi: 10.1016/s0360-3016(98)00341-1.
22. Calabrese EJ, Dhawan G. How radiotherapy was historically used to treat pneumonia: could it be useful today? Yale J Biol Med. 2013; 86(4): 555–570, indexed in Pubmed: 24348219.
23. Arenas M, Sabater S, Hernández V, et al. Anti-inflammatory effects of low-dose radiotherapy. Indications, dose, and radiobiological mechanisms involved. Strahlenther Onkol. 2012; 188(11): 975–981, doi: 10.1007/s00066-012-0170-8, indexed in Pubmed: 22907572.